Stripe order manipulated dominant pairing symmetry in the Hubbard model

Chao Chen,[1,2] Zenghui Fan,[1] Runyu Ma ◉,[1,2] Yue Pan,[1] Ying Liang,[1,3] Bing Huang,[1,2,*] and Tianxing Ma[1,3,†]

[1]*Department of Physics, Beijing Normal University, Beijing 100875, China*
[2]*Beijing Computational Science Research Center, Beijing 100084, China*
[3]*Key Laboratory of Multiscale Spin Physics (Ministry of Education), Beijing Normal University, Beijing 100875, China*

Understanding the relationship between stripe order and other phenomena, including antiferromagnetism and superconductivity, is one of the central issues in cuprate superconductors. The discovery that similar phase diagram exhibits in both hole-doped and electron-doped cuprates brings a chance to explore the subtle role that stripe order plays in the mechanism of superconductivity. To investigate this question, we study the behavior of the superconducting pairing interaction within an inhomogeneous Hubbard model by the quantum Monte Carlo method. Our study shows that stripe order may play a different role in the electron-doped and hole-doped cases. For hole doping, the effective pairing interaction of dominant $d_{x^2-y^2}$ pairing symmetry can be enhanced by stripe potential V_0 at moderate hole-doping concentration, but suppressed by V_0 at low hole-doping regions. However, for electron doping, the effective pairing interaction of $d_{x^2-y^2}$ pairing symmetry is always suppressed by V_0. Surprisingly, when the dominant $d_{x^2-y^2}$ pairing disappears, there exists a robust d_{xy} pairing channel induced by V_0. Besides, with the occurrence of d_{xy} pairing, the (π, π) magnetic correlation is suppressed. In general, our unbiased numerical simulations provide an understanding of the superconducting mechanism in cuprate superconductors and offer possible evidence that the charge density waves have an important effect on superconductivity.

I. INTRODUCTION

Since the discovery of high temperature superconductivity (SC) in doped cuprates, there has been a strong emphasis on understanding the essential physics of high-T_c SC [1–6]. One major challenge arises from the intricate phase diagram, including the so-called pseudogap, strange-metal regimes and a variety of symmetry breaking orders [7–10]. Among them, charge density waves (CDWs) have been observed universally across different families of cuprates, but its interrelationship with superconductivity, antiferromagnetic and the pseudogap is still mysterious and interesting [3,11]. For example, the CDW order can coexist with superconductivity below the superconducting T_c, and its temperature dependence indicates a tendency to compete with superconductivity [12,13]. Besides, in YBa$_2$Cu$_3$O$_{6+x}$, high magnetic fields can enhance the CDW order and suppress superconductivity [14–16]. Nonetheless, on theoretical grounds it has been suggested that charge order may play an important positive role in the mechanism of high-T_c SC [17–20]. Actually, by using scanning tunneling microscopy, researchers find the charge order exhibits clear positive correlation with cooper pairing modulation in doped Bi$_2$Sr$_2$CaCu$_2$O$_{8+\delta}$ [21]. The recent experiments also indicate that the CDW order not only competes with SC but also assists it in superconductor NbSe$_2$ [22] and UTe$_2$ [23].

Although the analogous forms of charge order and superconducting pairing symmetry have been observed in both electron- and hole-doped cuprates, there are obviously many differences between them [3,10,24–26]. For instance, the hole-doped compounds have apical oxygens. On contrary, the electron-doped cuprates are characterized by a lack of apical oxygens [27]. Superconductivity in the electron-doped cuprates appears in a very narrow doping range ($0.13 \leqslant \delta_e \leqslant 0.2$); in the hole-doped case the range is broader ($0.05 \leqslant \delta_h \leqslant 0.3$) [3,10,28]. The highest T_c values of hole-doped cuprates are apparently higher than that of electron-doped counterparts [3,10,25]. These novel phenomenon raise two interesting questions: What causes the difference between electron-doped and hole-doped cuprates? More specifically, are the effects of CDWs on the superconducting mechanism similar or different between hole-doped cuprates and electron doped cuprates? Therefore comparing the difference among them may provide an unexpected perspective to reveal the interplay between symmetry-breaking order and superconductivity.

In this paper, we undertake a systematic quantum Monte Carlo study about the pairing correlation to uncover the effect of charge stripes in both hole- and electron-doped cases. For hole-doping regimes, even the existence of preformed stripe potential V_0, the $d_{x^2-y^2}$ pairing symmetry is still robust at different doping concentration. Moreover, we discover that the effective pairing interaction of $d_{x^2-y^2}$ pairing symmetry is enhanced by V_0 at hole-doping $\delta_h \approx 0.25$, but suppressed by V_0 at low hole-doping areas. Different from hole-doping cases, the $d_{x^2-y^2}$ pairing symmetry exhibits a complete instability at electron doping, which is suppressed by V_0 at whole

———————
*bing.huang@csrc.ac.cn
†txma@bnu.edu.cn
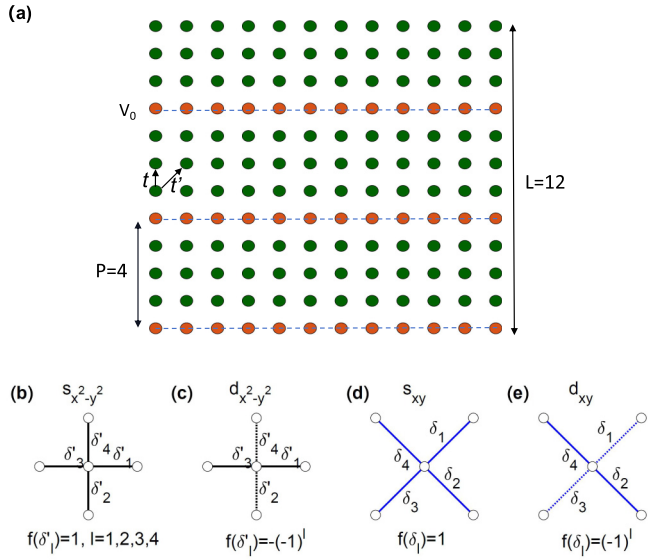
FIG. 1. (a) Geometry of the $L = 12$ square lattice with stripe period $\mathcal{P} = 4$. The red filled circles label the site with stripe potential V_0, and the green filled circles represent sites without V_0. t and t' denote hopping parameters. [(b)–(e)] Phase of the $s_{x^2-y^2}$, $d_{x^2-y^2}$, s_{xy}, and d_{xy}.

electron-doping regions. As V_0 increases, the dominant $d_{x^2-y^2}$ pairing symmetry is quickly disappeared, and replaced by d_{xy} pairing symmetry. Our results indicate that this d_{xy} pairing symmetry occurs with the appearance of charge stripe. Additionally, when we consider the charge inhomogeneity at electron-doping cases, the AFM correlation is suppressed with the enhancement of V_0. Our discovery may provide a perspective to grasp the interplay between charge order and other phenomena (for example, antiferromagnetism and superconductivity) and highlight the difference between electron-doped and hole-doped cuprates.

II. MODEL AND METHODS

We study the two-dimensional repulsive Hubbard model on a square lattice. The Hamiltonian is

$$
\hat{H} = -t \sum_{\langle \mathbf{i}, \mathbf{j} \rangle \sigma} c_{\mathbf{i}\sigma}^{\dagger} c_{\mathbf{j}\sigma} - t' \sum_{\langle\langle \mathbf{i}, \mathbf{j} \rangle\rangle \sigma} c_{\mathbf{i}\sigma}^{\dagger} c_{\mathbf{j}\sigma} + U \sum_{\mathbf{i}} n_{\mathbf{i}\uparrow} n_{\mathbf{i}\downarrow}
$$
$$
- \mu \sum_{\mathbf{i}} (n_{\mathbf{i}\uparrow} + n_{\mathbf{i}\downarrow}) + V_0 \sum_{i_y \in \mathcal{P}} (n_{\mathbf{i}\uparrow} + n_{\mathbf{i}\downarrow}). \quad (1)
$$

Here, $c_{\mathbf{i}\sigma}$ ($c_{\mathbf{i}\sigma}^{\dagger}$) annihilates (creates) electrons at site $\mathbf{i}$ with spin σ ($\sigma = \uparrow, \downarrow$), and $n_{\mathbf{i}\sigma} = c_{\mathbf{i}\sigma}^{\dagger} c_{\mathbf{i}\sigma}$ is the particle-number operator for spin σ. $\mathbf{i}, \mathbf{j}$ and $\langle\langle \mathbf{i}, \mathbf{j} \rangle\rangle$ denote nearest- and next-nearest neighbors, respectively. We set nearest-neighbor hopping t as the energy unit, and the t' is next-nearest-neighbor hopping. The doping level is obtained by varying chemical potential μ. V_0 is an additional site potential exerted on a set of rows $\mathbf{i} = (i_x, i_y)$ with $mod(i_y, \mathcal{P}) = 0$, i.e., red filled circles in Fig. 1(a). We choose $\mathcal{P} = 4$ to grasp the stripe-ordered patterns of cuprates observed experimentally [11,29]. Here, we emphasize that V_0 is phenomenological. And, it has no direct microscopic origin corresponding to actual parameter in

the materials. We also note that this model does not resolve the issue of spontaneous stripe formation in a broken translational symmetry system, but it allows us to check the characteristic of magnetic and pairing correlations when the system exhibits a set of preformed stripes with reduced particle density. In fact, it is an appropriate approximation model when the energy scale of striped order formation is bigger than that of superconductivity [30–33], which is true in both electron-doped and hole-doped cuprates [3,11,34].

Our simulations are mainly performed on the lattice shown in Fig. 1(a) by using the determinant quantum Monte Carlo (DQMC) method with periodic boundary conditions. The main idea of the finite temperature DQMC algorithm is to convert the interacting fermion model into the system of free fermions coupled with auxiliary field. Specifically, by employing the Suzuki-Trotter decomposition, partition function $Z = \text{Tr} \exp(-\beta H)$ is expressed in a discretized imaginary-time slice, and then the four-fermions interactions term in Hamiltonian is decoupled by standard Hubbard-Stratonovich (HS) transformation. In the process, the errors caused by the Trotter decomposition are proportional to $(\Delta\tau)^2$, where $\Delta\tau$ is time slice. Therefore the errors can be made sufficiently small by decreasing $\Delta\tau$. And we set $\Delta\tau = 0.1$ to ensure systematic errors smaller than those associated with statistical sampling [35]. Finally, tracing out fermions can be executed since only quadratic fermion operators appear in the exponential of partition function. In our calculations, 6000 warm-up sweeps are used to equilibrate the system and additional 12 000–48 000 sweeps are conducted for measurements, which are split into 20 bins. For more technical details about DQMC, please see Refs. [36–40]

To investigate the superconducting property under charge-density modulation, we define the pairing susceptibility,

$$
P_\alpha = \frac{1}{N_s} \sum_{\mathbf{i}, \mathbf{j}} \int_0^\beta d\tau \langle \Delta_\alpha^{\dagger}(\mathbf{i}, \tau) \Delta_\alpha(\mathbf{j}, 0) \rangle, \quad (2)
$$

where α denotes the pairing symmetry. Due to the constraint of Coulomb repulsion U in Eq. (1), pairing between two sublattices is favored. The corresponding order parameter $\Delta_\alpha^{\dagger}(\mathbf{i})$ is written as

$$
\Delta_\alpha^{\dagger}(\mathbf{i}) = \sum_l f_\alpha^{\dagger}(\delta_l)(c_{\mathbf{i}\uparrow} c_{\mathbf{i}+\delta_l \downarrow} - c_{\mathbf{i}\downarrow} c_{\mathbf{i}+\delta_l \uparrow})^{\dagger},
$$

where $f_\alpha(\delta_{\mathbf{l}})$ represents the form factor of pairing function. The vectors $\delta_{\mathbf{l}}$ and $\delta_{\mathbf{l}}'$ denote nearest- and next-nearest-neighbor connections, respectively, which are pictured in Figs. 1(b)–1(e). Considering the structure of square lattice, the possible pairing forms are given by (a) $s_{x^2-y^2}$, (b) $d_{x^2-y^2}$, (c) s_{xy}, and (d) d_{xy} [32,41]. These different pairing symmetries have the following form factor:

$$
s_{x^2-y^2}\text{-wave}: f_{s_{x^2-y^2}}(\delta_l) = 1, \ l = 1, 2, 3, 4,
$$
$$
d_{x^2-y^2}\text{-wave}: f_{d_{x^2-y^2}}(\delta_l) = 1(\delta_l = (\pm\hat{x}, 0)),
$$
$$
\text{and} f_{d_{x^2-y^2}}(\delta_l) = -1(\delta_l = (0, \pm\hat{y}));
$$
$$
s_{xy}\text{-wave}: f_{s_{xy}}(\delta_l') = 1, \ l = 1, 2, 3, 4,
$$
$$
d_{xy}\text{-wave}: f_{d_{xy}}(\delta_l') = 1(\delta_l' = \pm(-\hat{x}, \hat{y})),
$$
$$
\text{and} f_{d_{xy}}(\delta_l') = -1(\delta_l' = \pm(\hat{x}, \hat{y})). \quad (3)
$$
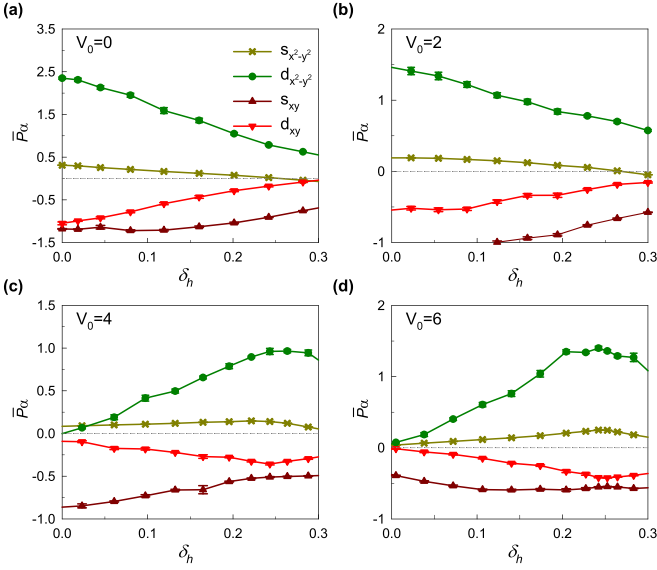
FIG. 2. The effective pairing interaction $\bar{P}_\alpha$ as a function of hole doping δ_h at $T = 1/6$ and $U/t = 4.0$ on a $L = 12$ lattice for the different stripe potential (a) $V_0 = 0$, (b) 2, (c) 4, and (d) 6.

FIG. 3. The effective pairing interaction $\bar{P}_\alpha$ as a function of electron-doping δ_e at $T = 1/6$ and $U/t = 4.0$ on a $L = 12$ lattice for the different stripe potential (a) $V_0 = 0$, (b) 2, (c) 4, and (d) 6.

In fact, the effective pairing interaction serves as a stronger evidence for identifying the dominant superconducting pairing symmetry [42–44]. To obtain the effective pairing interaction $\bar{P}_\alpha$ in finite system, the uncorrelated single-particle contribution $\widetilde{P}_\alpha(\mathbf{i}, \mathbf{j})$ is also calculated, which is achieved by replacing $\langle c^\dagger_{\mathbf{i}\downarrow} c_{\mathbf{j}\downarrow} c^\dagger_{\mathbf{i}+\delta_l\uparrow} c_{\mathbf{j}+\delta_{l'}\uparrow} \rangle$ in Eq. (2) with $\langle c^\dagger_{\mathbf{i}\downarrow} c_{\mathbf{j}\downarrow} \rangle \langle c^\dagger_{\mathbf{i}+\delta_l\uparrow} c_{\mathbf{j}+\delta_{l'}\uparrow} \rangle$. Subsequently, we get the effective pairing interaction $\bar{P}_\alpha = P_\alpha - \widetilde{P}_\alpha$. Our DQMC simulations yield negative effective pairing interaction and pairing susceptibility, which reflects the pairing symmetry is suppressed by other competing pairing channels or phases [42–44]. On the contrary, the positive pairing interaction suggests that there is indeed the possibility of superconductivity driven by electron-electron correlation.

Furthermore, in order to explore the magnetic excitation, we calculate the spin susceptibility in the z direction at zero frequency,

$$\chi(q) = \frac{1}{N_s} \int_0^\beta d\tau \sum_{\mathbf{i},\mathbf{j}} e^{iq \cdot (\mathbf{i}-\mathbf{j})} \langle \mathrm{m}_{\mathbf{i}}(\tau) \cdot \mathrm{m}_{\mathbf{j}}(0) \rangle, \qquad (4)$$

where $m_{\mathbf{i}}(\tau) = e^{H\tau} m_{\mathbf{i}}(0) e^{-H\tau}$ with $m_{\mathbf{i}} = c^\dagger_{\mathbf{i}\uparrow} c_{\mathbf{i}\uparrow} - c^\dagger_{\mathbf{i}\downarrow} c_{\mathbf{i}\downarrow}$.

III. RESULTS AND DISCUSSION

In this work, we mainly discuss the system with a set of preformed charge stripes under $\mathcal{P} = 4$, simulating the effects of the charge density modulation. We have calculated the hole-doping dependence of the effective pairing interaction $\bar{P}_\alpha$ at $T = 1/6$ and $U/t = 4.0$ with different stripe potential strengths in Fig. 2. As shown in Fig. 2(a), when the system is homogeneous ($V_0 = 0$), the $d_{x^2-y^2}$ pairing symmetry is always robust at different doping levels and becomes biggest at the zero doping, which is associated with strong scattering by the antiferromagnetic background [41,45]. Once the system is
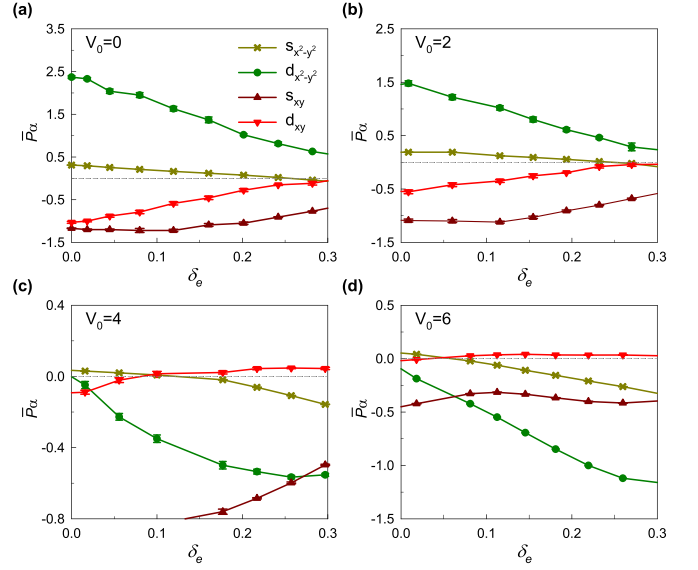
doped away from half filling, the uncorrelated single-particle contribution $\widetilde{P}_\alpha$ increases when temperature is lowered [41]. In Figs. 2(a)–2(d), with the enhancement of stripe potential, the effective pairing interaction of $d_{x^2-y^2}$ pairing symmetry is clearly decreased at low doping region and becomes very small for $V_0 \geqslant 4$ at low doping area. On the contrary, we can notice that $\bar{P}_\alpha(d_{x^2-y^2})$ is enhanced at hole-doping level $\delta_h \approx 0.25$ as V_0 increases, and a clear peak is observed at $\delta_h \approx 0.25$ in Fig. 2(c) and 2(d). This enhancement might be caused by the appearance of more nearly half-filled regions between stripes for large V_0 at $\delta_h \approx 0.25$ [32,33]. Besides, we can also observe that the preformed stripe potential under $\mathcal{P} = 4$ may not cause the change of dominant superconducting pairing symmetry for hole doping.

Despite the abundance of experimental and theoretical studies of charge order and SC in the hole-doped cuprates, comprehensive studies of the electron-doped compounds are much less [3,10,24–26]. To distinguish the difference between hole-doped and electron-doped cases, more detailed simulations about the latter are presented in the following. As shown in Figs. 3(a) and 3(b), the $\bar{P}_\alpha(d_{x^2-y^2})$ is quickly decreased as V_0 increases at all electron-doping levels. Intriguingly, in Figs. 3(c) and 3(d), we can notice that the effective pairing interactions of $d_{x^2-y^2}$ wave becomes negative in all electron-doping region, reflecting the fact that the $d_{x^2-y^2}$ pairing symmetry is totally suppressed. On the contrary, the effective pairing interaction with the d_{xy} pairing symmetry becomes positive in large electron-doping levels, although its numerical value is relatively small. All of this indicates that the $d_{x^2-y^2}$ pairing symmetry is not always robust under the presence of charge-density modulation at electron doping, and there might be a transition from dominant $d_{x^2-y^2}$ pairing symmetry to d_{xy} pairing symmetry, induced by charge inhomogeneity. Besides, combining Figs. 2(a) and 3(a), we can notice that the effective pairing interaction of $d_{x^2-y^2}$ pairing channel exhibits symmetry about zero doping. However, as
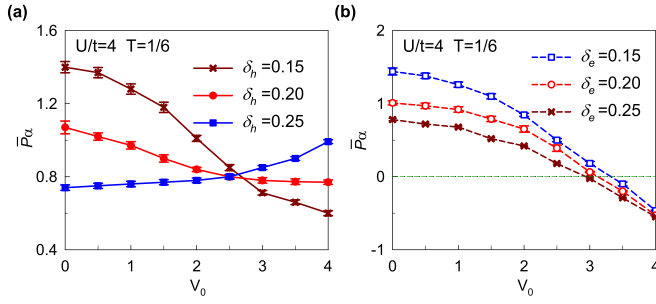
FIG. 4. $\bar{P}_\alpha(d_{x^2-y^2})$ as a function of V_0 for (a) different hole-doping concentration and (b) different electron-doping concentration at $T = 1/6$ and $U/t = 4.0$ on a $L = 12$ lattice.

V_0 increases, it breaks particle-hole symmetry and then the symmetry about $\bar{P}_\alpha$ disappears.

Moreover, Fig. 4 directly shows $\bar{P}_\alpha(d_{x^2-y^2})$ as a function of V_0 at hole-doped and electron-doped cases. For hole doping in Fig. 4(a), it is clearly to see that the effective pairing interaction with $d_{x^2-y^2}$ symmetry is always positive in the parameter range. With the enhancement of V_0, $\bar{P}_\alpha(d_{x^2-y^2})$ exhibits a strong doping dependence. Specifically, $\bar{P}_\alpha(d_{x^2-y^2})$ for $\delta_h = 0.25$ is stably enhanced as V_0 increases. However, with the increase of V_0, $\bar{P}_\alpha(d_{x^2-y^2})$ is decreased at $\delta_h = 0.20$ and 0.15. This directly indicates stripe potential has a complex relationship with the dominant $d_{x^2-y^2}$ wave at hole-doping case. Besides, comparing results of $\delta_h = 0.20$ and 0.15, we can get that stripe potential has a larger inhibitory effect on superconductivity at lower hole-doping concentration. This is consistent with Fig. 2. For the electron-doped case in Fig. 4(b), we can notice that $d_{x^2-y^2}$ pairing channel is always suppressed by V_0 at all typical electron-doped levels. Meanwhile, $\bar{P}_\alpha(d_{x^2-y^2})$ quickly becomes negative at large V_0, which reflects the vanish of dominant $d_{x^2-y^2}$ wave.

Comparing the difference between hole-doped and electron-doped cases, we can get that the preformed stripe potential exhibits both positive and negative influence on the $d_{x^2-y^2}$ pairing channel at hole doping, but always negative effect at electron-doping case. Additionally, the stripe potential has a stronger inhibitory effect on $d_{x^2-y^2}$ wave at electron-doped case, which may relate to why SC in the electron-doped cuprates appears in a smaller narrow doping range and has lower T_c values than hole-doped cuprates. Actually, our calculations under striped period $\mathcal{P} = 8$ also support that the charge stripe modulation indeed has a stronger inhibitory effect on $d_{x^2-y^2}$ pairing symmetry at electron doping than hole doping (Figs. 8 and 9).

To further clarify the role of V_0 in electron-doped case, we mainly discuss the behavior of the effective pairing interaction at typical electron-doping $\delta_e = 0.2$, where the sign problem [40,46] is relatively friendly in Fig. 10. As shown in Figs. 5(a) and 5(b), when $V_0 = 4$ or 6, the effective pairing interaction for d_{xy} pairing symmetry increases with decreasing temperature, but other pairing symmetries quickly decrease as temperature is lowered, which indicates the d_{xy} wave is possibly robust for moderate stripe potential strength at electron-doped area. In Fig. 5(c), we show the temperature dependence of $\bar{P}_\alpha(d_{xy})$ for different stripe potential strengths at electron-doping $\delta_e = 0.2$ with $U/t = 4.0$. We can clearly
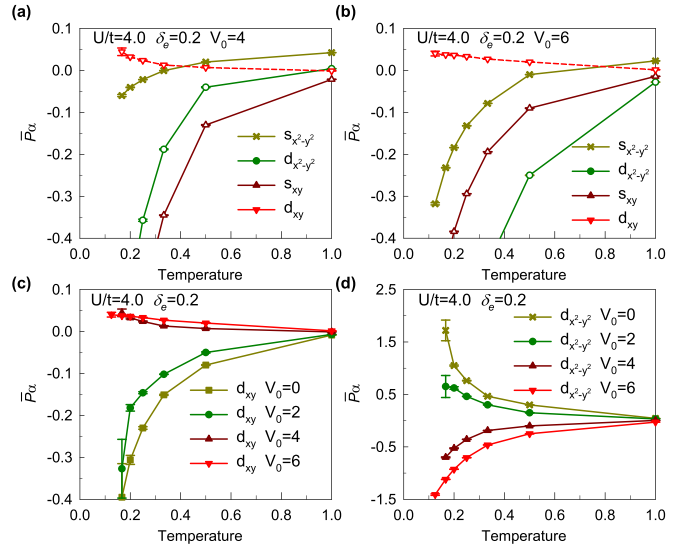
FIG. 5. The effective pairing interaction $\bar{P}_\alpha$ as a function of temperature for different pairing symmetries at electron-doping $\delta_e = 0.2$ and $U/t = 4$ on a $L = 12$ lattice when (a) $V_0 = 4$ and (b) 6. (c) $\bar{P}_\alpha(d_{xy})$, (d) The $\bar{P}_\alpha(d_{x^2-y^2})$ as a function of temperature for different V_0 at electron-doping $\delta_e = 0.2$ and $U/t = 4$ on a $L = 12$ lattice.

observe that the d_{xy} pairing symmetry is enhanced with the increasing of V_0. This change from being inhibited to being facilitated is quite surprising. However, in Fig. 5(d), the $\bar{P}_\alpha(d_{x^2-y^2})$ exhibits different temperature dependence, which is always suppressed by stripe potential. Moreover, this suppressive effect is enhanced with increasing V_0 or decreasing temperature, demonstrating the instability of $d_{x^2-y^2}$ pairing symmetry under charge stripe phase at electron doping. Our further calculations show that this d_{xy} pairing symmetry is robust at different interaction strengths or lattice sizes. Later, in Fig. 11, we check the interaction dependence and size dependence of $\bar{P}_\alpha(d_{xy})$.

Recently, there is growing evidence that the next-nearest hopping t' plays a significant role in revealing the interplay between superconductivity and charge density wave and spin density wave orders [47–50]. In Fig. 6, we consider the effect of t' on pairing interaction. As shown in Fig. 6(a), the $\bar{P}_\alpha(d_{xy})$ is visibly suppressed by negative t', but insensitive
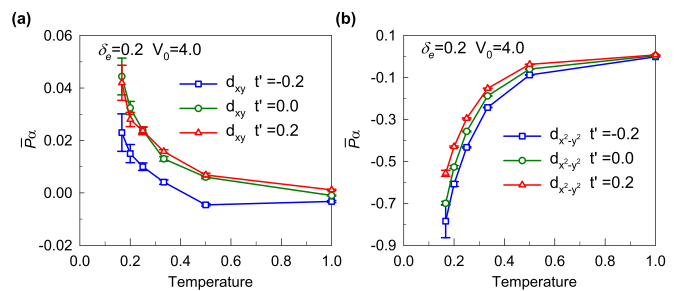
FIG. 6. The effective pairing interaction of (a) d_{xy} pairing symmetry, (b) $d_{x^2-y^2}$ pairing symmetry as a function of temperature for different next-nearest hopping t' at electron-doping $\delta_e = 0.2$, $V_0 = 4$ and $U/t = 4$ on a $L = 12$ lattice.
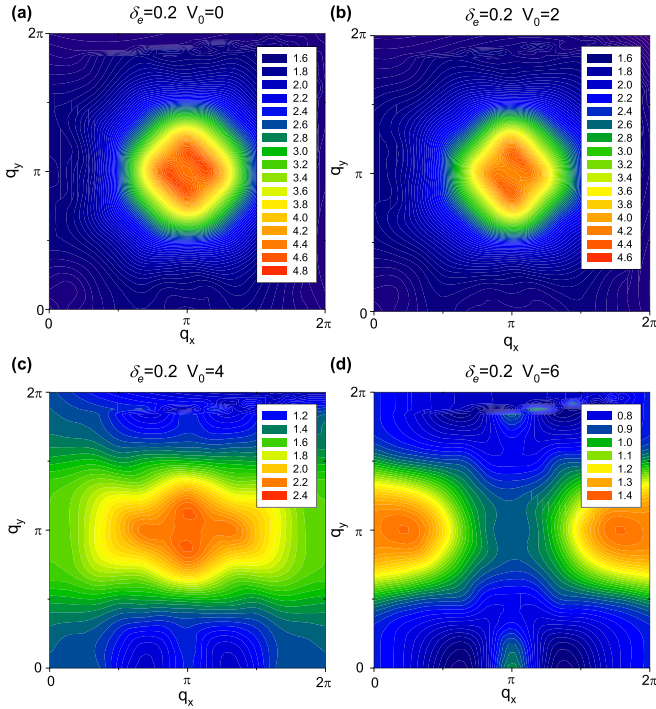
FIG. 7. The spin susceptibility $\chi(q)$ in the first Brillouin zone at electron-doping $\delta_e = 0.2$, $T = 1/6$, $U/t = 4.0$ for the different stripe potential (a) $V_0 = 0$, (b) 2, (c) 4, and (d) 6.

FIG. 8. The effective pairing interaction $\bar{P}_\alpha$ as a function of hole doping δ_h with stripe period $\mathcal{P} = 8$ at $T = 1/6$ and $U/t = 4.0$ on a $L = 16$ lattice for the different stripe potential (a) $V_0 = 1$, (b) 2, (c) 4, and (d) 6.

to positive t' within the parameters calculated. In Fig. 6(b), we can see that $\bar{P}_\alpha(d_{x^2-y^2})$ is slightly enhanced by positive t'. Even including the next-nearest-neighbor hopping, the d_{xy} pairing symmetry is still dominant and $d_{x^2-y^2}$ pairing symmetry is suppressed at $V_0 = 4$ and $\delta_e = 0.2$. Due to the limitation at lower temperatures, more efficient techniques are needed to identify whether the d_{xy} wave is still robust in the ground state. Later, in Fig. 12, we also study the effect of t' on hole-doped case with $V_0 = 4$, which supports negative t' can apparently enhance $d_{x^2-y^2}$ pairing in the hole-doped system.

Besides the characteristics of pairing interaction, it is also interesting to investigate the role of charge stripe on the modulation of spin correlation. In Fig. 7, we compare the obtained spin susceptibility $\chi(q)$ for different stripe potential V_0 at electron-doping $\delta_e = 0.2$. One can notice that the (π, π) magnetic correlation is decreased as V_0 increases. When $V_0 = 4$ and 6, the antiferromagnetic fluctuation disappears, which is accompanied by $d_{x^2-y^2}$ wave being inhibited and d_{xy} wave being promoted in Figs. 5(c) and 5(d). Considering that magnetism and superconductivity simultaneously exhibit different properties with increasing stripe potential strength, we suggest that the dominant pairing symmetry is also strongly interwoven with magnetic properties of the system.

IV. SUMMARY

In summary, we mainly study the superconducting behavior of a two-dimensional inhomogeneous Hubbard model with striped charge-density-wave modulation at period
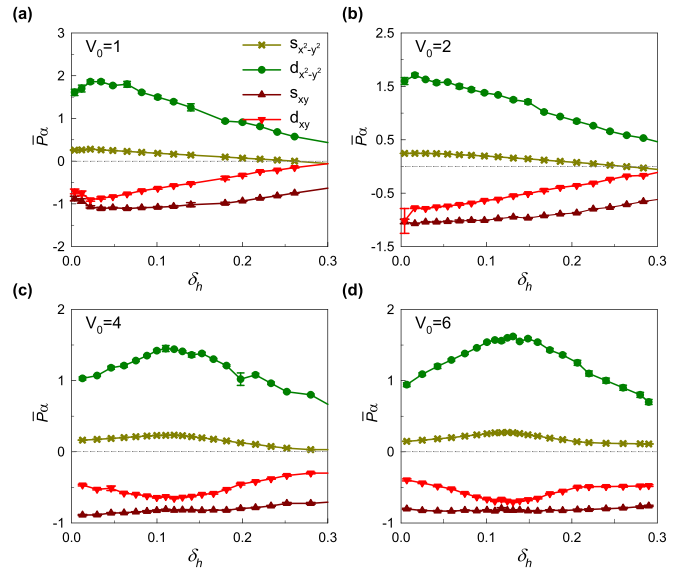
$\mathcal{P} = 4$, using the DQMC method. From our calculations, we can discover that stripe potential has a complex relationship with the $d_{x^2-y^2}$ pairing symmetry at hole doping, but only competition with it at electron doping. In other words, the pairing correlation of $d_{x^2-y^2}$ pairing channel is easily suppressed by stripe order at electron-doped case, which may matter why SC in the electron-doped cuprates occurs in a smaller narrow doping range with lower T_c values than hole-doped cuprates. Furthermore, in the electron-doped system, we find a dominant d_{xy} pairing symmetry, which is induced by charge stripe and always robust under different U, L, and t'. Although previous experiments support predominantly d-wave symmetry in the cuprates, it is still controversial about its pairing mechanism, especially in electron-doped cuprates [3,28,34,51]. Therefore, in the mixed phase of electron-doped cuprates, more experiments may be needed to distinguish d_{xy} and $d_{x^2-y^2}$ pairings. Besides, accompanied by the transition of dominant pairing symmetry at electron-doped cases, the (π, π) magnetic correlation is suppressed. Thus, our calculations are possibly important to understand the unconventional pairing mechanism of copper-based superconductors, and reveal the difference about pairing mechanism between electron-doped and hole-doped cuprates.
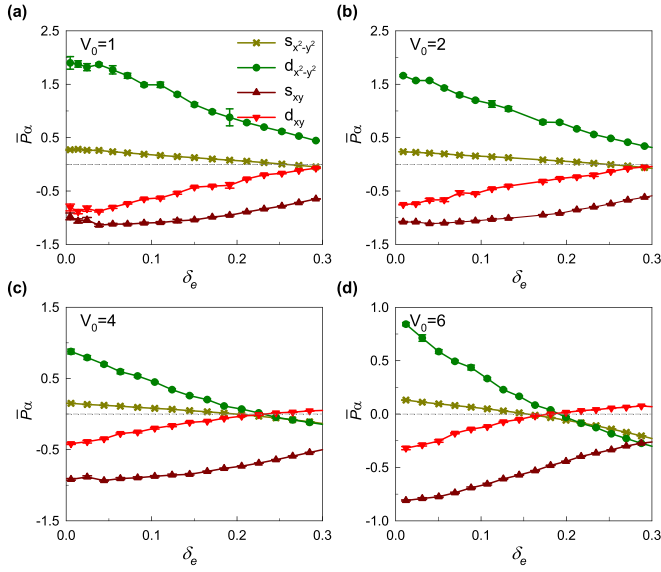
FIG. 9. The effective pairing interaction $\bar{P}_\alpha$ as a function of electron-doping δ_e with stripe period $\mathcal{P} = 8$ at $T = 1/6$ and $U/t = 4.0$ on a $L = 16$ lattice for the different stripe potential (a) $V_0 = 1$, (b) 2, (c) 4, and (d) 6.

APPENDIX A: PAIRING INTERACTION UNDER STRIPED PERIOD $\mathcal{P} = 8$

Previous findings supported striped order with wavelength $\lambda \approx 8$ in the ground state of the 1/8-hole-doped Hubbard model under $t' = 0$ [52]. Therefore we have also studied the effect of charge stripes with wavelength 8. As shown in Fig. 8, we have calculated the hole-doping dependence of $\bar{P}_\alpha$ with striped period $\mathcal{P} = 8$ for the different stripe potential. With the increase of V_0, the effective pairing interaction of $d_{x^2-y^2}$ pairing symmetry is clearly decreased at most hole-doping concentration. However, $\bar{P}_\alpha(d_{x^2-y^2})$ is slightly enhanced at hole-doping level $\delta_h \approx 0.125$, and a peak is observed at $\delta_h \approx 0.125$ in Figs. 8(c) and 8(d). It is observed that $d_{x^2-y^2}$ pairing symmetry is always robust for $V_0 = 0 \sim 6$ under $\mathcal{P} = 8$. However, when it comes to electron-doped case in Fig. 9, we can clearly notice that $\bar{P}_\alpha(d_{x^2-y^2})$ is always decreased at all electron-doping concentration as V_0 increases. When V_0 increases to 4 and 6 in Figs. 9(c) and 9(d), we can see that $\bar{P}_\alpha(d_{x^2-y^2})$ becomes negative at large electron-doping concentration, supporting the fact that the $d_{x^2-y^2}$ wave is totally suppressed. On the contrary, the effective pairing interaction with the d_{xy} pairing symmetry becomes positive at such electron-doping levels. Considering the results of $\mathcal{P} = 4$ and $\mathcal{P} = 8$, we can conclude that the stripe potential exhibits both positive and negative influence on the $d_{x^2-y^2}$ wave at hole doping. For electron-doped case, $d_{x^2-y^2}$ pairing channel is always suppressed by stripe potential. Overall, the stripe potential indeed has a stronger inhibitory effect on $d_{x^2-y^2}$ wave at electron doping than hole doping under both $\mathcal{P} = 4$ and 8.

APPENDIX B: THE SIGN PROBLEM

In our simulations, we have performed an analysis about the infamous sign problem [40] under the mainly
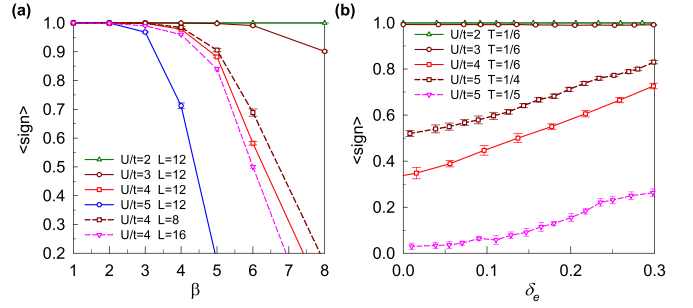
FIG. 10. (a) Average sign $\langle sign \rangle$ versus the inverse temperatures $\beta = 1/T$ for different interaction strengths or lattice sizes at electron-doping $\delta_e = 0.2$ and $V_0 = 4$. (b) $\langle sign \rangle$ as a function of electron-doping δ_e for different interaction strength or temperature at $V_0 = 4$ on a $L = 12$ lattice.

calculated parameters. In Fig. 10(a), $\langle sign \rangle$ quickly decreases when the inverse temperature exceeds 4. From Fig. 10, one can also notice that the sign problem becomes worse for higher interaction strength or larger lattice size, which makes it difficult to research in low temperatures and strong-coupling cases. To keep quality of data, the average sign is larger than 0.45 in main simulations. Moreover, much longer measurements 12 000–48 000 are performed to compensate the fluctuations when sign problem is much worse [36]. These efforts ensure the reliability and accuracy of our results.

APPENDIX C: DIFFERENT U OR L

Figure 11(a) shows the effective pairing interaction $\bar{P}_\alpha(d_{xy})$ as a function of temperature for different interaction strengths. The d_{xy} pairing channel is always robust at different interaction strength and $\bar{P}_\alpha(d_{xy})$ is enhanced with increasing U, indicating the importance of electron-electron correlation. Figure 11(b) suggests that lattice size effect of $\bar{P}_\alpha(d_{xy})$ is very weak, i.e., $L = 8$, 12, and 16 exhibit almost identical results, suggesting our result is well converged and reliable.
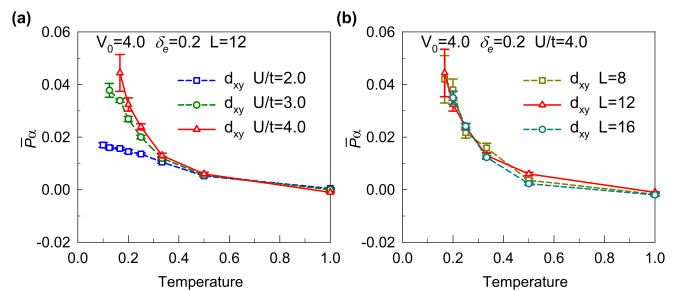
FIG. 11. The effective pairing interaction $\bar{P}_\alpha(d_{xy})$ as a function of temperature (a) for different interaction strength at electron-doping $\delta_e = 0.2$ and $V_0 = 4.0$ on a $L = 12$ lattice, (b) for different lattice sizes at electron-doping $\delta_e = 0.2$, $V_0 = 4.0$, and $U/t = 4.0$.
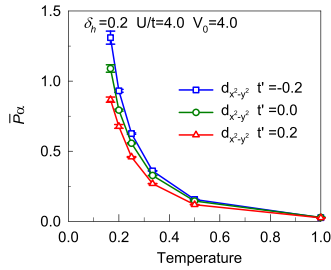
FIG. 12. The effective pairing interaction of $d_{x^2-y^2}$ pairing symmetry as a function of temperature for different next-nearest hopping t' at hole-doping $\delta_h = 0.2$, $V_0 = 4$, and $U/t = 4$ on a $L = 12$ lattice.

APPENDIX D: EFFECT OF t' FOR HOLE-DOPED CASE

Despite the influence of t' and V_0, $d_{x^2-y^2}$ pairing symmetry is always dominant at hole-doped case. In Fig. 12, we have calculated the temperature-dependent $\bar{P}_\alpha(d_{x^2-y^2})$ for different t' at hole-doping $\delta_h = 0.2$. As the temperature is lowered, $\bar{P}_\alpha(d_{x^2-y^2})$ will increase rapidly. Notably, it is observed that the $\bar{P}_\alpha(d_{x^2-y^2})$ is enhanced by the negative t' but suppressed by positive t', suggesting the important role of t' at hole-doped case. Actually, this enhancement is in agreement with previous observation that next-nearest hopping t' is negative in hole-doped cuprates [53]. Besides, recent work also supports that the negative t' can enhance superconductivity in the hole-doped Hubbard model [47].

[1] J. G. Bednorz and K. A. Müller, Possible high T$_c$ superconductivity in the Ba−La−Cu−O system, Z. Phys. B **64**, 189 (1986).

[2] L. F. Schneemeyer, J. V. Waszczak, T. Siegrist, R. B. van Dover, L. W. Rupp, B. Batlogg, R. J. Cava, and D. W. Murphy, Superconductivity in YBa$_2$Cu$_3$O$_7$ single crystals, Nature (London) **328**, 601 (1987).

[3] C. C. Tsuei and J. R. Kirtley, Pairing symmetry in cuprate superconductors, Rev. Mod. Phys. **72**, 969 (2000).

[4] J. Hwang, T. Timusk, and J. P. Carbotte, Scanning-tunnelling spectra of cuprates, Nature (London) **446**, E3 (2007).

[5] X. Zhou, W.-S. Lee, M. Imada, N. Trivedi, P. Phillips, H.-Y. Kee, P. Törmä, and M. Eremets, High-temperature superconductivity, Nat. Rev. Phys. **3**, 462 (2021).

[6] S.-Di Chen, M. Hashimoto, Y. He, D. Song, J.-F. He, Y.-F. Li, S. Ishida, H. Eisaki, J. Zaanen, T. P. Devereaux, D.-H. Lee, D.-H. Lu, and Z.-X. Shen, Unconventional spectral signature of T$_c$ in a pure d-wave superconductor, Nature (London) **601**, 562 (2022).

[7] C. M. Varma, P. B. Littlewood, S. Schmitt-Rink, E. Abrahams, and A. E. Ruckenstein, Phenomenology of the normal state of Cu−O high-temperature superconductors, Phys. Rev. Lett. **63**, 1996 (1989).

[8] V. J. Emery and S. A. Kivelson, Frustrated electronic phase separation and high-temperature superconductors, Physica C: Superconductivity **209**, 597 (1993).

[9] S. A. Kivelson, G. Aeppli, and V. J. Emery, Thermodynamics of the interplay between magnetism and high-temperature superconductivity, Proc. Natl. Acad. Sci. USA **98**, 11903 (2001).

[10] P. A. Lee, N. Nagaosa, and X.-G. Wen, Doping a mott insulator: Physics of high-temperature superconductivity, Rev. Mod. Phys. **78**, 17 (2006).

[11] R. Comin and A. Damascelli, Resonant x-ray scattering studies of charge order in cuprates, Annu. Rev. Condens. Matter Phys. **7**, 369 (2016).

[12] G. Ghiringhelli, M. L. Tacon, M. Minola, S. Blanco-Canosa, C. Mazzoli, N. B. Brookes, G. M. De Luca, A. Frano, D. G. Hawthorn, F. He, T. Loew, M. M. Sala, D. C. Peets, M. Salluzzo, E. Schierle, R. Sutarto, G. A. Sawatzky, E. Weschke, B. Keimer, and L. Braicovich, Long-range incommensurate charge fluctuations in (Y, Nd)Ba$_2$Cu$_3$O$_{6+x}$, Science **337**, 821 (2012).

[13] E. H. da Silva Neto, P. Aynajian, A. Frano, R. Comin, E. Schierle, E. Weschke, A. Gyenis, J. Wen, J. Schneeloch, Z. Xu, S. Ono, G. Gu, M. L. Tacon, and A. Yazdani, Ubiquitous interplay between charge ordering and high-temperature superconductivity in cuprates, Science **343**, 393 (2014).

[14] T. Wu, H. Mayaffre, S. Krämer, M. Horvatić, C. Berthier, W. N. Hardy, R. Liang, D. A. Bonn, and M.-H. Julien, Magnetic-field-induced charge-stripe order in the high-temperature superconductor YBa$_2$Cu$_3$O$_y$, Nature (London) **477**, 191 (2011).

[15] J. Chang, E. Blackburn, A. T. Holmes, N. B. Christensen, J. Larsen, J. Mesot, R. Liang, D. A. Bonn, W. N. Hardy, A. Watenphul, M. v. Zimmermann, E. M. Forgan, and S. M. Hayden, Direct observation of competition between superconductivity and charge density wave order in YBa$_2$Cu$_3$O$_{6.67}$, Nat. Phys. **8**, 871 (2012).

[16] S. Gerber, H. Jang, H. Nojiri, S. Matsuzawa, H. Yasumura, D. A. Bonn, R. Liang, W. N. Hardy, Z. Islam, A. Mehta, S. Song, M. Sikorski, D. Stefanescu, Y. Feng, S. A. Kivelson, T. P. Devereaux, Z.-X. Shen, C.-C. Kao, W.-S. Lee, D. Zhu, and et al., Three-dimensional charge density wave order in YBa$_2$Cu$_3$O$_{6.67}$ at high magnetic fields, Science **350**, 949 (2015).

[17] C. Castellani, C. Di Castro, and M. Grilli, Singular quasiparticle scattering in the proximity of charge instabilities, Phys. Rev. Lett. **75**, 4650 (1995).

[18] E. Arrigoni, E. Fradkin, and S. A. Kivelson, Mechanism of high-temperature superconductivity in a striped Hubbard model, Phys. Rev. B **69**, 214519 (2004).

[19] T. Ying, R. Mondaini, X. D. Sun, T. Paiva, R. M. Fye, and R. T. Scalettar, Determinant quantum Monte Carlo study of d-wave pairing in the plaquette Hubbard Hamiltonian, Phys. Rev. B **90**, 075121 (2014).

[20] H.-C. Jiang and S. A. Kivelson, Stripe order enhanced superconductivity in the Hubbard model, Proc. Natl. Acad. Sci. USA **119**, e2109406119 (2022).

[21] W. Ruan, X. Li, C. Hu, Z. Hao, H. Li, P. Cai, X. Zhou, D.-H. Lee, and Y. Wang, Visualization of the periodic modulation of cooper pairing in a cuprate superconductor, Nat. Phys. **14**, 1178 (2018).

[22] K. Cho, M. Kończykowski, S. Teknowijoyo, M. A. Tanatar, J. Guss, P. B. Gartin, J. M. Wilde, A. Kreyssig, R. J. McQueeney, A. I. Goldman, V. Mishra, P. J. Hirschfeld, and R. Prozorov, Using controlled disorder to probe the interplay between charge

order and superconductivity in NbSe$_2$, Nat. Commun. **9**, 2796 (2018).

[23] A. Aishwarya, J. May-Mann, A. Raghavan, L. Nie, M. Romanelli, S. Ran, S. R. Saha, J. Paglione, N. P. Butch, E. Fradkin, and V. Madhavan, Magnetic-field-sensitive charge density waves in the superconductor UTe$_2$, Nature (London) **618**, 928 (2023).

[24] E. Dagotto, Correlated electrons in high-temperature superconductors, Rev. Mod. Phys. **66**, 763 (1994).

[25] D. J. Scalapino, A common thread: The pairing interaction for unconventional superconductors, Rev. Mod. Phys. **84**, 1383 (2012).

[26] E. Fradkin, S. A. Kivelson, and J. M. Tranquada, Colloquium: Theory of intertwined orders in high temperature superconductors, Rev. Mod. Phys. **87**, 457 (2015).

[27] C. Weber, K. Haule, and G. Kotliar, Strength of correlations in electron- and hole-doped cuprates, Nat. Phys. **6**, 574 (2010).

[28] N. P. Armitage, P. Fournier, and R. L. Greene, Progress and perspectives on electron-doped cuprates, Rev. Mod. Phys. **82**, 2421 (2010).

[29] E. H. da Silva Neto, R. Comin, F. He, R. Sutarto, Y. Jiang, R. L. Greene, G. A. Sawatzky, and A. Damascelli, Charge ordering in the electron-doped superconductor Nd$_{2-x}$Ce$_x$CuO$_4$, Science **347**, 282 (2015).

[30] T. A. Maier, G. Alvarez, M. Summers, and T. C. Schulthess, Dynamic cluster quantum Monte Carlo simulations of a two-dimensional Hubbard model with stripelike charge-density-wave modulations: Interplay between inhomogeneities and the superconducting state, Phys. Rev. Lett. **104**, 247001 (2010).

[31] I. Martin, D. Podolsky, and S. A. Kivelson, Enhancement of superconductivity by local inhomogeneities, Phys. Rev. B **72**, 060502(R) (2005).

[32] R. Mondaini, T. Ying, T. Paiva, and R. T. Scalettar, Determinant quantum Monte Carlo study of the enhancement of d-wave pairing by charge inhomogeneity, Phys. Rev. B **86**, 184506 (2012).

[33] L. Zhang, T. Guo, Y. Mou, Q. Chen, and T. Ma, Enhancement of d-wave pairing in the striped phase with nearest neighbor attraction, Phys. Rev. B **105**, 155154 (2022).

[34] J. A. Sobota, Y. He, and Z.-X. Shen, Angle-resolved photoemission studies of quantum materials, Rev. Mod. Phys. **93**, 025006 (2021).

[35] R. Mondaini, K. Bouadim, T. Paiva, and R. R. dos Santos, Finite-size effects in transport data from quantum Monte Carlo simulations, Phys. Rev. B **85**, 125127 (2012).

[36] R. Blankenbecler, D. J. Scalapino, and R. L. Sugar, Monte Carlo calculations of coupled boson-fermion systems. I, Phys. Rev. D **24**, 2278 (1981).

[37] S. R. White, D. J. Scalapino, R. L. Sugar, E. Y. Loh, J. E. Gubernatis, and R. T. Scalettar, Numerical study of the two-dimensional Hubbard model, Phys. Rev. B **40**, 506 (1989).

[38] T. Ma, L. Zhang, C.-C. Chang, H.-H. Hung, and R. T. Scalettar, Localization of interacting dirac fermions, Phys. Rev. Lett. **120**, 116601 (2018).

[39] L. Zhang, T. Ma, N. C. Costa, R. R. dos Santos, and R. T. Scalettar, Determinant quantum Monte Carlo study of exhaustion in the periodic anderson model, Phys. Rev. B **99**, 195147 (2019).

[40] R. Mondaini, S. Tarat, and R. T. Scalettar, Quantum critical points and the sign problem, Science **375**, 418 (2022).

[41] S. R. White, D. J. Scalapino, R. L. Sugar, N. E. Bickers, and R. T. Scalettar, Attractive and repulsive pairing interaction vertices for the two-dimensional Hubbard model, Phys. Rev. B **39**, 839 (1989).

[42] T. Ma, H.-Q. Lin, and J. Hu, Quantum Monte Carlo study of a dominant s-wave pairing symmetry in iron-based superconductors, Phys. Rev. Lett. **110**, 107002 (2013).

[43] T. Huang, L. Zhang, and T. Ma, Antiferromagnetically ordered mott insulator and d + id superconductivity in twisted bilayer graphene: a quantum Monte Carlo study, Sci. Bull. **64**, 310 (2019).

[44] C. Chen, R. Ma, XueLei Sui, Y. Liang, B. Huang, and T. Ma, Antiferromagnetic fluctuations and dominant d_{xy}-wave pairing symmetry in nickelate-based superconductors, Phys. Rev. B **106**, 195112 (2022).

[45] K. Liu, S. Yang, W. Li, T. Ying, J. Yang, X. Sun, and X. Li, The pairing symmetries in the two-dimensional Hubbard model, Phys. Lett. A **392**, 127153 (2021).

[46] E. Y. Loh, J. E. Gubernatis, R. T. Scalettar, S. R. White, D. J. Scalapino, and R. L. Sugar, Sign problem in the numerical simulation of many-electron systems, Phys. Rev. B **41**, 9301 (1990).

[47] H.-C. Jiang and T. P. Devereaux, Superconductivity in the doped Hubbard model and its interplay with next-nearest hopping t', Science **365**, 1424 (2019).

[48] P. Mai, N. S. Nichols, S. Karakuzu, F. Bao, A. Del Maestro, T. A. Maier, and S. Johnston, Robust charge-density-wave correlations in the electron-doped single-band Hubbard model, Nat. Commun. **14**, 2889 (2023).

[49] H. Xu, C.-M. Chung, M. Qin, U. Schollwöck, S. R. White, and S. Zhang, Coexistence of superconductivity with partially filled stripes in the Hubbard model, arXiv:2303.08376.

[50] Y.-F. Jiang, T. P. Devereaux, and H.-C. Jiang, Ground state phase diagram and superconductivity of the doped Hubbard model on six-leg square cylinders, arXiv:2303.15541.

[51] Y. Li, W. Tabis, Y. Tang, G. Yu, J. Jaroszynski, N. Barišić, and M. Greven, Hole pocket-driven superconductivity and its universal features in the electron-doped cuprates, Sci. Adv. **5**, eaap7349 (2019).

[52] B.-X. Zheng, C.-M. Chung, P. Corboz, G. Ehlers, M.-P. Qin, R. M. Noack, H. Shi, S. R. White, S. Zhang, and G. K.-L. Chan, Stripe order in the underdoped region of the two-dimensional Hubbard model, Science **358**, 1155 (2017).

[53] A. Damascelli, Z. Hussain, and Z.-X. Shen, Angle-resolved photoemission studies of the cuprate superconductors, Rev. Mod. Phys. **75**, 473 (2003).